

## Durham Research Online

---

### Deposited in DRO:

16 May 2018

### Version of attached file:

Accepted Version

### Peer-review status of attached file:

Peer-reviewed

### Citation for published item:

Robinson, T. (2018) 'Road impacts from the 2016 Kaikura earthquake : an analogue for a future Alpine Fault earthquake?', New Zealand journal of geology and geophysics., 61 (3). pp. 403-411.

### Further information on publisher's website:

<https://doi.org/10.1080/00288306.2018.1470539>

### Publisher's copyright statement:

This is an Accepted Manuscript of an article published by Taylor Francis in New Zealand Journal of Geology and Geophysics on 21 May 2018, available online: <http://www.tandfonline.com/10.1080/00288306.2018.1470539>.

### Additional information:

---

### Use policy

The full-text may be used and/or reproduced, and given to third parties in any format or medium, without prior permission or charge, for personal research or study, educational, or not-for-profit purposes provided that:

- a full bibliographic reference is made to the original source
- a [link](#) is made to the metadata record in DRO
- the full-text is not changed in any way

The full-text must not be sold in any format or medium without the formal permission of the copyright holders.

Please consult the [full DRO policy](#) for further details.

# Road impacts from the 2016 Kaikōura earthquake: an analogue for a future Alpine Fault earthquake?

Tom R Robinson

Department of Geography, Durham University, Durham, UK

[Tom.robinson@durham.ac.uk](mailto:Tom.robinson@durham.ac.uk)

## Abstract

The 2016  $M_w$  7.8 Kaikōura earthquake involved complex rupture of multiple faults for > 170 km, generating strong ground shaking throughout the upper South Island leading to widespread landsliding. As a result of surface fault rupture and landslides, State Highway 1 and State Highway 70 were blocked, isolating Kaikōura and the surrounding communities and necessitating evacuations by air and sea. In all these respects the Kaikōura earthquake can be considered an analogue for a future Alpine Fault earthquake, providing lessons for the necessary emergency response. Landslide blockages primarily occurred where surrounding slopes averaged > 18° and where Peak Ground Acceleration was > 0.43 g, Peak Ground Velocity > 41 cm/s, or Modified Mercalli Intensity > 7.9. Using a potential future Alpine Fault scenario earthquake, this study identifies locations on other key state highway routes that have similar predictive variables that may therefore become blocked in a future earthquake. This suggests that SH6 between Hokitika and Haast, State Highway 73 near Arthur's Pass, and State Highway 94 south of Milford Sound are all likely to be affected. This will necessitate the evacuation of large numbers of spatially distributed tourists as well as the resupply of isolated local populations. The possibility of bad weather along with a lack of sea ports south of Hokitika will likely make such activities challenging. Contingency planning based on experiences from the Kaikōura earthquake is therefore necessary and likely to prove invaluable following an Alpine Fault earthquake.

**Keywords:** Earthquakes, Landslides, Hazard modelling, Risk analysis, Emergency response.

## 1 INTRODUCTION

The 14 November 2016  $M_w$  7.8 Kaikōura earthquake was the largest to strike New Zealand since 2009. The earthquake involved complex rupture of over 20 previously known and unknown faults in the upper South Island (Hamling et al., 2017) and propagated > 170 km north from the epicentre near Waiau (Fig. 1). With rupture initiating at a depth of just 15 km, the earthquake resulted in strong ground shaking (> 1g) throughout the upper South Island and lower North Island (Kaiser et al., 2017). The affected region is steep and mountainous, rising from sea-level to over 2,500 m in ~20 km. Consequently, > 10,000 landslides are thought to have occurred resulting in > 190 landslide dams (Massey et al., 2018). Despite its mountainous nature, the region is an important transport corridor linking Christchurch, Kaikōura, Blenheim, and Picton via State

Highway (SH) 1. Consequently, the earthquake caused substantial impacts in the form of landslides and surface fault rupture blocking SH1, causing Kaikōura to be cut-off from the rest of the South Island. These road blockages resulted in the road being closed for ~1 year (Mason et al. 2017), although closures due to heavy rainfall and further landsliding continue to occur at the time of writing. A full description of the damage caused by the event has been summarised by numerous authors in an NZSEE Special Issue (e.g. Orense et al., 2017; Cubrinovski et al., 2017; Palermo et al., 2017; Liu et al., 2017).

The impacts from the Kaikōura earthquake are in many respects a potential analogue for the impacts resulting from a future rupture of the Alpine Fault (Fig. 1). This oblique strike-slip fault runs along the western edge of the Southern Alps for c. 411 km ( $\pm 10\%$ ) and forms the onshore plate boundary between the Australian and Pacific plates, sustaining a slip rate of  $27 \pm 5$  mm/yr. The Alpine Fault has generated large ( $M_w 8.1 \pm 0.2$ ) earthquakes regularly over the last 8,000 years, with a relatively invariable average recurrence of ~341 years or less (Berryman et al., 2012; Stirling et al., 2012; Howarth et al., 2016; Cochran et al., 2017). The last known Alpine Fault earthquake occurred in 1717 AD (Yetton, 1998; Wells et al., 1999; Howarth et al., 2012; De Pascale & Langridge, 2012) giving an ~26% conditional probability of rupture in the next 50 years (Biasi et al., 2015). Such an earthquake is expected to be  $M_w \sim 8.0$ , have a rupture length > 200 km, initiate at shallow (<15 km) depth and, consequently, generate strong ground shaking throughout the affected area (Fig. 1) resulting in widespread landsliding (Robinson & Davies, 2013; Robinson et al., 2016). Like the Kaikōura area, the West Coast Region, where the Alpine Fault is located, forms a narrow coastal strip between the Tasman Sea and the Southern Alps. The region is rural, sparsely populated, and relatively inaccessible: only one road (SH6) traverses the region, and only three roads (SH6, SH7, & SH73) cross the Southern Alps connecting it with the rest of the South Island (Fig. 1). These routes navigate through steep and narrow Alpine Passes (Arthur's Pass, Lewis Pass and Haast Pass) and cross the Alpine Fault at multiple locations. Consequently, there is a potential for substantial disruption to these routes from landslides and other ground damage triggered by an Alpine Fault earthquake. Thus, despite significant differences in the seismological factors between the Kaikōura earthquake and a future Alpine Fault earthquake, the former presents an opportunity to learn from its impacts and the subsequent emergency response and formulate effective response and recovery plans for a future Alpine Fault earthquake.

Using observations of road impacts from the 2016 Kaikōura earthquake, this study aims to envisage the potential road impacts resulting from a future rupture of the Alpine Fault. The conditions under which road blockages resulted in the Kaikōura event are investigated and subsequently an analysis of where similar conditions exist along road networks is undertaken. Using a scenario Alpine Fault earthquake, the locations where roads are liable to blockages are identified along with any resulting isolated areas. Reflecting on the experience of the Kaikōura earthquake, a discussion of the potential emergency response requirements is provided.

## 77    **2 METHODS & DATA**

78    The primary form of road impacts in the Kaikōura earthquake resulted from fault rupture and  
79    landslides (Mason et al., 2017; Davies et al., 2017; Stirling et al., 2017; Dellow et al., 2017). By  
80    assessing the locations where road impacts occurred in this event, it may be possible to identify  
81    sections of road elsewhere in the South Island with similar conditions that may therefore suffer  
82    impacts in a future earthquake on other faults (e.g. the Alpine Fault). This study uses road  
83    blockage data collected by NZTA in the immediate aftermath of the Kaikōura earthquake and is  
84    therefore assumed to have resulted from the mainshock only. The data captures full and partial  
85    blockages of major public roads but does not include data on private roads or 4x4 tracks. The  
86    study area encompasses the region outlined in Fig. 1, which captures the region of South Island  
87    exposed to shaking greater than MMI 6.

### 89    **2.1 Fault rupture impacts**

90    Due to the number and complexity of surface fault ruptures in the Kaikōura earthquake (Stirling et  
91    al., 2017), multiple sections of both SH1 and SH70 were directly affected by surface fault rupture  
92    (Fig. 1). Where surface ruptures intersected these roads, the road surface was displaced, with  
93    vertical displacements in particular making the road impassable (see Stirling et al., 2017 and  
94    Davies et al., 2017 for examples). Identifying potential sites of future fault rupture impacts for an  
95    Alpine Fault earthquake requires identifying locations where other roads intersect the proposed  
96    surface rupture trace. Given uncertainties in accurately locating a fault surface trace, this study  
97    considers any road within 50 m of the known surface trace of the Alpine Fault to be potentially  
98    affected by surface fault rupture. It should be highlighted however, that such an approach is only  
99    applicable for known faults and surface traces. During the Kaikōura earthquake, surface fault  
100    rupture occurred on several previously unknown faults and fault traces (Stirling et al., 2017). Fault  
101    rupture impacts for a future Alpine Fault earthquake scenario must therefore be considered as a  
102    minimum assessment, with further impacts from currently unknown faults possible.

### 104    **2.2 Landslide impacts**

105    While assessing road impacts from surface fault rupture requires a simple analysis of the locations  
106    where roads and faults intersect, identifying potential locations for landslide impacts is more  
107    difficult. During the Kaikōura earthquake, landslide road impacts occurred as a result of slippage  
108    as well as falling debris (Dellow et al., 2017; Davies et al., 2017). Identifying road sections exposed  
109    to landslide impacts therefore requires identifying both where landslide source areas may occur, as  
110    well as their corresponding runout paths, which is a difficult and time-consuming task. One way to  
111    simplify this is to assess the values of landslide predictor variables in proximity to roads and  
112    compare sections that were blocked because of earthquake-induced landslides in a previous  
113    earthquake with those that were unaffected. Such an approach can allow mean threshold values of  
114    various predictor variables above which all, or the majority, of blockages may occur.

115 The most important predictor variables for landslide occurrence have previously been  
116 shown to be some measure of ground shaking (such as Peak Ground Acceleration, PGA), local  
117 hillslope gradient and local geology (Parker et al., 2015). This study assesses the average slope  
118 angle and ground shaking surrounding roads affected by the 2016 Kaikōura earthquake in order to  
119 identify the threshold values above which landslide road impacts occurred. Geology is not  
120 considered as most slope failures occurred in greywacke which is the dominant rock type in the  
121 area (Massey et al. 2018). This assumes that slopes comprised of schist along the West Coast,  
122 where the Alpine Fault is located, will perform similarly to the greywacke slopes north and south of  
123 Kaikōura.

124 Ground shaking can be measured using a variety of different variables, including Peak  
125 Ground Acceleration (PGA), Peak Ground Velocity (PGV) and Modified Mercalli Intensity (MMI). All  
126 three measures of ground shaking are compared for the Kaikōura earthquake (Fig. 1) using data  
127 from Bradley et al. (2017a) at 1 km grid resolution. It should be noted however, that the shaking  
128 values for the Kaikōura earthquake from Bradley et al. (2017a) differ from those derived by the  
129 USGS and ShakeMap NZ models. Nevertheless, scenario outputs for an Alpine Fault earthquake  
130 from the USGS and ShakeMap NZ are not available, while outputs using the same model as  
131 Bradley et al. (2017a) are available (Bradley et al., 2017b, c); this study therefore uses the Bradley  
132 et al. (2017a) outputs to maintain consistency. Slope angle is calculated from the Land Information  
133 New Zealand DEM using a grid size of 25 m. It should be noted however, that such a resolution is  
134 likely to be coarse to identify small artificial slopes such as road cuts. While these slopes present a  
135 notable and local hazard, Mason et al. (2017) highlight that in the Kaikōura earthquake road cut  
136 failures were limited to minor rockfall which predominantly resulted in minor impingement of the  
137 road course or the blockage of a single lane. This may not, however, be the case for an Alpine  
138 Fault earthquake.

139 Affected roads are split into 500 m segments and buffers of 100 m, 250 m, and 500 m are  
140 created around each segment. A length of 500 m was chosen to provide a reasonable resolution  
141 whilst allowing consistent analysis when applied to the much larger study area for the Alpine Fault  
142 earthquake scenario. Buffer widths are selected primarily to account for short-, medium-, and long-  
143 landslide runout lengths, with few landslides having runouts > 500 m (Massey et al., 2017). Buffer  
144 widths < 100 m are assumed to be meaningful due to the pixel resolution of 25 m. Mean  
145 values of ground shaking and slope angle are calculated within each buffer zone and values  
146 relating to blocked and unblocked road sections are compared.

147

### 148 **2.3 An Alpine Fault earthquake scenario**

149 In order to identify potential locations of road impacts from a future Alpine Fault earthquake, first a  
150 possible scenario earthquake must be derived. For this study, the scenario used in Project AF8  
151 ([www.projectaf8.co.nz](http://www.projectaf8.co.nz)) has been selected. Project AF8 aims to inform emergency response  
152 planning using scenario-based analysis. The scenario developed involves an  $M_w$  7.9 earthquake

153 with ~350 km rupture between Charles Sound and Hokitika (Fig. 1). Ground shaking variables for  
154 this scenario have been taken from Bradley et al. (2017b,c) at 1 km grid resolution. The effect of  
155 rupture directivity has been considered as part of Project AF8, with three different rupture  
156 directions considered: south-to-north, bi-lateral, and north-to-south. In this study, only the south-to-  
157 north rupture direction has been considered (Fig. 1) as, at the time of writing, it is the only scenario  
158 for which shaking data is openly available. Slope data is calculated using the same dataset and  
159 resolution as the Kaikōura dataset for consistency.

160

## 161 **3 RESULTS**

### 162 **3.1 Observed blockages from the Kaikōura earthquake**

163 Surface fault rupture crossed SH1 and SH70 at eight locations (Fig. 1). Five of these are located  
164 on SH1 as a result of surface rupture on the Kekerengu, Papatea, and Hundalee faults, and three  
165 on SH70 from the The Humps, North and South Leader, and Conway-Charwell faults (Stirling et  
166 al., 2017). Placing a 50 m buffer around the fault ruptures yields 10 locations, with the two extra  
167 locations occurring west of Oaro on SH70 where fault rupture ran parallel and close to the road  
168 (Fig. 1). This suggests that a 50 m buffer for the Alpine Fault scenario is appropriate although  
169 conservative.

170 Results for the analysis of landslide blockages show there were 20 blocked locations (Fig.  
171 2). Notably, regardless of buffer width, all road segments affected by landslides had surrounding  
172 slope angles that averaged  $> 17^\circ$  and shaking that averaged  $> 0.43$  g (PGA),  $> 41$  cm/s (PGV), or  
173  $MM > 7.9$  (MMI) (Fig. 2). By comparison, road segments with mean slope angle and ground  
174 shaking values that exceed these thresholds in the scenario Alpine Fault earthquake can therefore  
175 be considered at risk of landslide blockage. However, a large number of unblocked road segments  
176 also had average slope angles and ground shaking in excess of these thresholds (Fig. 2).

177 To optimise the predictive power of the model, higher thresholds are assigned that  
178 simultaneously maximise the number of blocked sections and minimise the number of unblocked  
179 sections above both thresholds. The upper threshold slope angle varies with buffer width, with  $22^\circ$   
180 for 100 m buffers,  $28^\circ$  for 250 m buffers, and  $25^\circ$  for 500 m buffers. For the ground shaking  
181 variables, buffer width has no effect on upper threshold values, with 0.56 g for PGA, 76 cm/s for  
182 PGV, and 8.8 for MMI respectively. If such thresholds were applied to other roads and earthquake  
183 scenarios (e.g., an Alpine Fault scenario), it would be possible, with uncertainty, to forecast  
184 locations where landslide blockages could be expected.

185 Before doing so, it is important to consider the predictive ability of each threshold  
186 combination, particularly in terms of the number of blockages (true positives) as well as the  
187 number of unblocked sections (false positives). For the Kaikōura earthquake, a total of 20 road  
188 sections were blocked, leaving 634 sections unblocked. A perfect prediction should therefore have  
189 all 20 blocked sections above the threshold combination and all 634 unblocked sections below.  
190 Data for the thresholds in Figure 2 are summarised in Table 1. The lower threshold combinations

for all buffer widths are deliberately set to successfully account for all 20 landslide blocked sections however, these thresholds also result in a large number of false positives, meaning the total number of blocked road sections are in the minority. For instance, using a 250 m buffer and PGA as the shaking predictor, a total of 56 road segments are above the lower thresholds, meaning just 36% were actually blocked (Table 1). Using the higher threshold combinations greatly reduces the number of false positives so that the majority of sections above the thresholds are true positives. However, this has the negative effect of reducing the total number of true positives. For instance, using the same example as before, 23 road segments are above the higher thresholds, of which 65% were actually blocked; however, 5 blocked segments are below the threshold combination.

### 3.2 Scenario Alpine Fault earthquake

For the scenario Alpine Fault earthquake (Fig. 1), seven sections of State Highway are located within 50 m of a known surface trace of the Alpine Fault (Fig. 3) and thus at risk of blockage in this scenario. The majority of these occur between the townships of Franz Josef and Haast, with a further location between Franz Josef and Hokitika. Surface fault ruptures from previous Alpine Fault earthquakes are thought to have averaged ~8 m horizontally and 1-2 m vertically (Berryman et al., 2012). Such displacements are similar to or larger than those experienced in the Kaikōura earthquake (Stirling et al., 2017) and suggest that these sections of road will be completely impassable to all vehicles.

The number and location of road segments exceeding the corresponding upper and lower landslide blockage thresholds from the Kaikōura earthquake (Fig. 2; Table 1) varies between 17 and 120 depending on the ground shaking variable and buffer width (Fig. 3). Using PGA consistently yields fewer segments at risk (between 17 and 24) of landslide blockages than PGV (between 54 and 91) or MMI (between 69 and 120). This appears to result from the lack of high PGA values in the Arthur's Pass region compared to high PGV and MMI values (Figs. 1 & 3). Without independent testing of the performance of each shaking variable it is impossible to say which performs best, however, the relative agreement between the PGV and MMI variables suggests the results associated with these measures may be more accurate.

In total, for the same shaking variable, the number of segments at risk of blockage generally decreases with decreasing buffer width. This likely relates the fact the majority of road segments for the Alpine Fault scenario are inland and therefore increases in buffer width produce larger changes in average slope angle than on the predominantly coastal roads affected by the Kaikōura event. Nevertheless, despite the variability, several sections of road are consistently at risk of landslide blockage, irrespective of the different buffer widths used. These are:

- SH6 immediately south of Franz Josef;
- SH6 ~20 km north-east of Haast;
- SH6 ~10 km east of Haast;
- SH94 immediately south of Milford Sound; and

- SH73 immediately north of Arthurs Pass.

If these sections were blocked, access to the West Coast Region would only be possible via SH7, with access only possible to ~50 km south of Hokitika. Consequently, according to the most recent NZ census (Statistics New Zealand, 2017), > 10,000 local people would be cut-off by road. Depending on the time of year, several thousand domestic and international tourists could also be affected. This is a substantially larger number of people than affected by the Kaikōura earthquake, with the population also being more widely distributed. Further, unlike during the Kaikōura earthquake when alternative access to Blenheim remained possible via SH7, no alternative road routes to Milford Sound, Franz Josef, Haast, or Arthur's Pass exist. Re-establishing connections with these townships is likely to prove a substantial challenge in both the short- and long-term following an Alpine Fault earthquake.

## **4 DISCUSSION**

### **4.1 Gaining emergency access**

Following the Kaikōura earthquake, CDEM immediately prioritised gaining access to isolated communities to provide essential supplies and evacuate stranded tourists in order to reduce the load on what limited local supplies were available (Davies et al., 2017). Due to road blockages, this was possible via only air and sea; however, both options proved unreliable. Poor weather conditions restricted flying and resulted in several days when flying was not possible, while the small size of, and damage to the Kaikōura port restricted the number and size of ships that could dock (Davies et al., 2017). In total 998 tourists were evacuated from Kaikōura either by air or by sea.

Similar issues are also expected to occur following an Alpine Fault earthquake. Gaining access to the West Coast Region and Milford Sound is likely to be CDEM's main priority, and with the expected damage to roads (Fig. 3), air and sea routes are likely to provide the only options. However, weather conditions west of the Southern Alps can be difficult and changeable, with monthly average rainfall in Hokitika averaging 250 mm while in Milford Sound this can exceed 500 mm, and with rainfall occurring > 200 days per year. Furthermore, few locations in West Coast Region have access to airstrips, meaning they are likely to be reliant on helicopters which have smaller weight carrying capacities than fixed wing aircraft. As in Kaikōura, ports in West Coast Region and Milford Sound are small and likely to have sustained damage during the earthquake, limiting the size and number of ships that can dock. However, no viable berthing spots for ships exist between Hokitika and Milford Sound, meaning isolated communities in this region are likely to be entirely reliant on air access.

A further complication exists in the number and location of tourists affected by an Alpine Fault earthquake. While ~1000 tourists were evacuated from Kaikōura following the 2016 earthquake, an Alpine Fault earthquake could affect far larger numbers of tourists. Over 1.3 million travellers visit the West Coast Region each year, with enough capacity for up to 4000 visitors per



night in the popular Franz Josef area (Tourism West Coast, 2015). Milford Sound is one of New Zealand's most popular tourist sites, attracting > 650,000 visitors per year, equating to ~1700 per day (Venture Southland, 2017). While at night visitors cluster to major townships, during the day most will be spread out across the region, with many visiting remote areas on foot. Consequently, it is possible that following an Alpine Fault earthquake, nearly five times as many tourists will require evacuation compared to the Kaikōura earthquake, with these people distributed across a region > 10,000 km<sup>2</sup>.

#### **4.2 Restoration and recovery**

New Zealand Transport Agency (NZTA) began clearing road blockages 2 days after the Kaikōura earthquake, focussing initially on SH70 and SH1 south of Kaikōura (Davies et al., 2017). The focus was primarily to return road access to all isolated communities and allow emergency vehicles access to affected regions. However, it took 11 days before non-emergency vehicles could leave Kaikōura via supervised convoy on SH70 (Davies et al., 2017). It took 23 days to restore supervised access to all isolated communities, with SH70 becoming the first road fully re-opened after 38 days. SH1 was finally re-opened in December 2017, albeit only to single-file traffic during daylight hours and in dry weather conditions.

Restoring road access following an Alpine Fault earthquake is likely to prove as difficult as the northern section of SH1. While access to the West Coast Region is likely to remain possible via SH7 (Fig. 3), restoring access along SH6 and SH73 is expected to prove difficult due to the steep terrain, likelihood of poor weather, and continuing aftershocks. Further considerations for restoration times include whether or not the road is confined, the volume of debris to remove and the ease of access. Reopening the alpine passes will prove most difficult, as the confined nature means rerouting the road is not an option and thus landslide debris will need to be removed. Further, the narrow nature of the passes means that debris clearance will likely be restricted to the outer-most blocking landslides, with limited options for simultaneous clearance of multiple landslide blockages. Previous estimates by NZTA have therefore suggested it would require > 6 months before restoration works could even begin on SH6 south of Franz Josef and east of Haast, and on SH73 (Robinson et al., 2015). Given the difficulties being experienced clearing SH1 north of Kaikōura these estimates appear to be realistic, if not under-estimates. This means no road access is expected on SH6 between Franz Josef and Haast, and along SH73 for > 6 months after an Alpine Fault earthquake. In comparison, SH94 is expected to be cleared within 14 days as the route is regularly blocked by avalanches and rockfalls and consequently NZTA are experienced at clearing this route and have sufficient equipment already in place (Robinson et al., 2015). It should be noted here however, that road bridge performance has not been accounted for here, and a collapse of a major road bridge is likely to present as large a challenge for restoration as landslide or surface fault rupture.

305 **4.3 Implications for emergency response**

306 The Kaikōura earthquake provides a useful analogue for a future Alpine Fault earthquake in terms  
307 of road impacts and loss of access. It therefore provides an opportunity to evaluate the emergency  
308 response undertaken and plan the necessary future response. Firstly, it is clear that planning for  
309 the evacuation of large numbers of spatially distributed tourists is essential. In the 2016  
310 earthquake, tourists were evacuated from Kaikōura township by a combination of air and sea, with  
311 363 evacuated by helicopter and 635 by sea (Davies et al., 2017). This evacuation was partly  
312 aided by tourists being concentrated in a single township, however in an Alpine Fault earthquake  
313 larger numbers of tourists are expected to be distributed across a much larger area, especially if it  
314 occurs during the daytime. This is in conjunction with an expectation that weather conditions in  
315 West Coast Region are likely to hinder air evacuations and the lack of sufficient port facilities will  
316 hinder evacuations by sea. It is therefore essential that contingency planning for the evacuation of  
317 tourists following an Alpine Fault earthquake is undertaken.

318 A further key issue is in the provision of emergency supplies to isolated local populations.  
319 While the current MCDEM advice is to be self-sufficient for 3 days following a disaster, it is clear  
320 that many West Coast communities will be isolated for far longer following an Alpine Fault  
321 earthquake. As in the Kaikōura earthquake, ensuring emergency supplies can be delivered to  
322 these regions is essential. While initially this may be able to be combined with evacuation of  
323 tourists, with some road routes expected to be impassable for > 6 months, continuous resupply by  
324 sea and air is unlikely to be sustainable. Considering alternative arrangements is therefore  
325 essential. One possibility is the temporary evacuation of isolated local populations until road  
326 access can be restored. However, this is likely to prove controversial and poses questions as to  
327 how to respond to anyone refusing to leave as well as the management of safe return. Planning  
328 how to maintain supplies to isolated locals for several months following an Alpine Fault earthquake  
329 is therefore urgently required.

330 A final implication to consider is the effect of such road impacts on the local economy. The  
331 West Coast Region has three major industries: mining, tourism, and dairy. Mining is predominantly  
332 dependant on the rail network, which has not been investigated in this study. However, the main  
333 rail route that transports mining products to Christchurch for national and international distribution  
334 follows SH73 for much of its route and therefore is also expected to be severely impacted. The  
335 loss of reliable road access to much of the region will undoubtedly affect the dairy and tourism  
336 industries, with farms unable to distribute milk products and tourists unable to reach popular  
337 destinations such as Franz Josef. While some work has been done to investigate the potential  
338 impact of an Alpine Fault earthquake on tourism (Orchiston, 2012), to date little work has looked at  
339 the potential impacts to the dairy industry.

340

341 **5 CONCLUSIONS**

In terms of its impacts, particularly to roads, the 2016 Kaikōura earthquake provides a potential analogue for a future rupture of the Alpine Fault. The 2016 Kaikōura earthquake displaced major state highways in several locations making the roads completely impassable. Numerous landslides also blocked key access routes, causing many communities to be isolated and requiring the evacuation of tourists by air and sea. An analysis of the predictive variables for landslide occurrence along the SH1 and SH70 road corridors show that the lower and upper thresholds respectively for road blockages were 15° and 28° for local slope, 0.43 g and 0.56 g for PGA, 41 cm/s and 76 cm/s for PGV, and 7.9 and 8.8 for MMI. Using these observations, this study identifies up to 120 other locations where landslides may potentially block roads in a future Alpine Fault earthquake. This suggests that blockages can be expected along SH6 between Hokitika and Haast, on SH94 before Milford Sound, and on SH73 around Arthur's Pass. Previous studies have suggested several sections of these roads could take > 6 months to restore. However, it is notable that the number of potential blockage sites varies considerably with different shaking variables, and the length of blockage time is dependent on numerous local factors, which this study has not investigated. Nevertheless, contingency planning for the evacuation of large numbers of spatially distributed tourists and the provision of sufficient emergency supplies to local populations is urgently required. Examining the response to the Kaikōura earthquake may therefore highlight valuable lessons that can be learnt prior to an Alpine Fault earthquake to aid such planning.

## ACKNOWLEDGEMENTS

I would like to acknowledge Dr Sam McColl and another anonymous reviewer whose helpful feedback greatly improved the quality and scope of this manuscript. This work was undertaken as part of funding provided by the EU Seventh Framework under the COFUND scheme with Durham University.

## REFERENCES

- Berryman, K. R., Cochran, U. A., Clark, K. J., Biasi, G. P., Langridge, R. M., & Villamor, P. (2012). Major earthquakes occur regularly on an isolated plate boundary fault. *Science*, 336(6089), 1690-1693.
- Biasi, G. P., Langridge, R. M., Berryman, K. R., Clark, K. J., & Cochran, U. A. (2015). Maximum-Likelihood Recurrence Parameters and Conditional Probability of a Ground-Rupturing Earthquake on the Southern Alpine Fault, South Island, New Zealand. *Bulletin of the Seismological Society of America*, 105(1), 94-106.
- Bradley, B. A., Razafindrakoto, H. N., & Polak, V. (2017) Ground motion observations from the 14 November 2016 Mw 7.8 Kaikōura, New Zealand, earthquake and insights from broadband simulations. *Seismological Research Letters*, 88, 740-756.
- Bradley, B. A., Bae, S. A., Polak, V., Lee, R. L., Thomson, E. M., & Tarbali, K. (2017b). Ground motion simulations of great earthquakes on the Alpine Fault: effect of hypocentre location and comparison with empirical modelling. *New Zealand Journal of Geology and Geophysics*, 60(3), 188–198.
- Bradley, B., A., Lagrava, D., Savarimuthu, S., & Bae S., E. (2017c). SeisFinder: A web application for the extraction of high-fidelity outputs from computationally-intensive earthquake resilience calculations. QuakeCoRE Annual Meeting, September 2017

382 Cochran, U. A., Clark, K. J., Howarth, J. D., Biasi, G. P., Langridge, R. M., Villamor, P., Berryman, K. R., & Vandergoes,  
383 M. J. (2017). A plate boundary earthquake record from a wetland adjacent to the Alpine fault in New Zealand refines  
384 hazard estimates. *Earth and Planetary Science Letters*, 464, 175-188.

385 Cubrinovski, M., Bray, J. D., de la Torre, C., Olsen, M. J., Bradley, B.A., Chiaro, G., Stocks, E., & Wotherspoon, L.,  
386 (2017). Liquefaction effects and associated damages observed at the Wellington Centreport from the 2016 Kaikōura  
387 earthquake. *Bulletin of the New Zealand Society for Earthquake Engineering*, 50(2), 152-173.

388 Davies, A. J., Sadashiva, V., Aghababaei, M., Barnhill, D., Costello, S. B., Fanslow, B., et al. (2017). Transport  
389 infrastructure performance and management in the South Island of New Zealand, during the first 100 days following  
390 the 2016 Mw 7.8 Kaikōura earthquake. *Bulletin of the New Zealand Society for Earthquake Engineering*, 50(2), 271-  
391 299.

392 De Pascale, G. P., & Langridge, R. M. (2012). New on-fault evidence for a great earthquake in AD 1717, central Alpine  
393 fault, New Zealand. *Geology*, 40(9), 791-794.

394 Dellow, S., Massey, C., Cox, S., Archibald, G., Begg, J., Bruce, Z., et al. (2017). Landslides caused by the 14 November  
395 2016 Mw7. 8 Kaikōura earthquake and the immediate response. *Bulletin of the New Zealand Society for Earthquake*  
396 *Engineering*, 50(2), 106-116.

397 Hamling, I. J., Hreinsdóttir, S., Clark, K., Elliott, J., Liang, C., Fielding, E., et al. (2017). Complex multifault rupture during  
398 the 2016 Mw 7.8 Kaikōura earthquake, New Zealand. *Science*, 356(6334).

399 Howarth, J. D., Fitzsimons, S. J., Norris, R. J., & Jacobsen, G. E. (2012). Lake sediments record cycles of sediment flux  
400 driven by large earthquakes on the Alpine fault, New Zealand. *Geology*, 40(12), 1091-1094.

401 Howarth, J. D., Fitzsimons, S. J., Norris, R. J., Langridge, R., Vandergoes, M. J. (2016). A 2000 yr rupture history for the  
402 Alpine fault derived from Lake Ellery, South Island, New Zealand. *Geological Society of America Bulletin*, 128, 627-  
403 643, doi:10.1130/B31300.1.

404 Kaiser, A., Balfour, N., Fry, B., Holden, C., Litchfield, N., Gerstenberger, M., et al. (2017). The 2016 Kaikōura, New  
405 Zealand, Earthquake: Preliminary Seismological Report. *Seismological Research Letters*, 88(3), 727-739.

406 Liu, Y., Nair, N-K., Renton, A., & Wilson, S. (2017). Impact of the Kaikōura earthquake on the electrical power system  
407 infrastructure. *Bulletin of the New Zealand Society for Earthquake Engineering*, 50(2), 300-305.

408 Mason, D., Brabhaharan, P. & Saul, G. (2017) Performance of road networks in the 2016 Kaikōura earthquake:  
409 Observations on ground damage and outage effects. Proc. 20th NZGS Geotechnical Symposium. Eds. GJ  
410 Alexander & CY Chin, Napier.

411 Massey, C., Townsend, D., Rathje, E., Allstadt, K. E., Lukovic, B., Kaneko, Y., Bradley, B., Wartman, J., Jibson, R. W.,  
412 Petley, D. N., Horspool, N., Hamling, I., Carey, J., Cox, S., Davidson, J., Dellow, S., Godt, J. W., Holden, C., Jones,  
413 K., Kaiser, A., Little, M., Lyndsell, B., McColl, S., Morgenstern, R., Rengers, F. K., Rhoades, D., Rosser, B., Strong,  
414 D., Singeisen, C., Villeneuve, M. (2017). Landslides Triggered by the 14 November 2016 MwMw 7.8 Kaikōura  
415 Earthquake, New Zealand. *Bulletin of the Seismological Society of America* doi: [https://doi-](https://doi-org.ezphost.dur.ac.uk/10.1785/0120170305)  
416 [org.ezphost.dur.ac.uk/10.1785/0120170305](https://doi-org.ezphost.dur.ac.uk/10.1785/0120170305)

417 Orchiston, C. (2012). Seismic risk scenario planning and sustainable tourism management: Christchurch and the Alpine  
418 Fault zone, South Island, New Zealand. *Journal of Sustainable Tourism*, 20(1), 59-79.

419 Orense, R. P., Mirjafari, Y., Asadi, S., Naghibi, M., Chen, X., Altaf, O., & Asadi, B. (2017). Ground performance in  
420 Wellington waterfront area following the 2016 Kaikōura earthquake. *Bulletin of the New Zealand Society for*  
421 *Earthquake Engineering*, 50(2), 142-151.

422 Palermo, A., Liu, R., Rais, A., McHaffie, B., Andisheh, K., Pampanin, S., Gentile, R., Nuzzo, I., Granerio, M., Loporcaro,  
423 G., McGann, C., & Wotherspoon, L. (2017). Performance of road bridges during the 14 November 2016 Kaikōura  
424 earthquake. *Bulletin of the New Zealand Society for Earthquake Engineering*, 50(2), 253-270.

425 Parker, R. N., Hancox, G. T., Petley, D. N., Massey, C. I., Densmore, A. L., & Rosser, N. J. (2015). Spatial distributions  
426 of earthquake-induced landslides and hillslope preconditioning in the northwest South Island, New Zealand. *Earth*  
427 *Surface Dynamics*, 3(4), 501.

428 Robinson, T. R., & Davies, T. R. H. (2013). potential geomorphic consequences of a future great (Mw= 8.0+) Alpine Fault  
 429 earthquake, South Island, New Zealand. *Natural Hazards and Earth System Sciences*, 13(9), 2279.  
 430 Robinson, T. R., Wilson, T. M., Buxton, R., Cousins, W. J., & Christophersen, A. M. (2015) An Alpine Fault earthquake  
 431 scenario to aid in the development of the Economics of Resilient Infrastructure's MERIT model. ERI Research  
 432 Report 2016/04.  
 433 Robinson, T. R., Davies, T. R. H., Wilson, T. M., & Orchiston, C. (2016). Coseismic landsliding estimates for an Alpine  
 434 Fault earthquake and the consequences for erosion of the Southern Alps, New Zealand. *Geomorphology*, 263, 71-  
 435 86.  
 436 Statistics New Zealand (2017). Subnational population estimates: at 30 June 2017 (provisional). Retrieved from  
 437 nzdotstat.stats.govt.nz/wbos/Index.aspx?DataSetCode=TABLECODE7541. Last Accessed 28 March 2018.  
 438 Stirling, M., McVerry, G., Gerstenberger, M., Litchfield, N., Van Dissen, R., Berryman, K., Barnes, P., Wallace, L.,  
 439 Villamor, P., Langridge, R., Lamarche, G., Nodder, S., Reyners, M., Bradley, B., Rhoades, D., Smith, W., Nicol, A.,  
 440 Pettinga, J., Clark, K., Jacobs, K. (2012). National Seismic Hazard Model for New Zealand: 2010 Update. *Bulletin of*  
 441 *the Seismological Society of America*, 102 (4): 1514–1542. doi: <https://doi.org/10.1785/0120110170>  
 442 Stirling, M. W., Litchfield, N. J., Villamor, P., Van Dissen, R. J., Nicol, A., Pettinga, J., et al. (2017). The Mw7. 8 2016  
 443 Kaikōura earthquake: Surface fault rupture and seismic hazard context. *Bulletin of the New Zealand Society for*  
 444 *Earthquake Engineering*, 50(2), 73-84.  
 445 Tourism West Coast (2015) Minutes of the Annual General Meeting of Tourism West Coast Inc. 5<sup>th</sup> July 2015.  
 446 Venture Southland (2017) Southland tourism key indicators. MBIE Report.  
 447 Wells, A., Yetton, M. D., Duncan, R. P., & Stewart, G. H. (1999). Prehistoric dates of the most recent Alpine fault  
 448 earthquakes, New Zealand. *Geology*, 27(11), 995-998.  
 449 Yetton, M. D. (1998). Progress in understanding the paleoseismicity of the central and northern Alpine Fault, Westland,  
 450 New Zealand. *New Zealand Journal of Geology and Geophysics*, 41(4), 475-483.  
 451



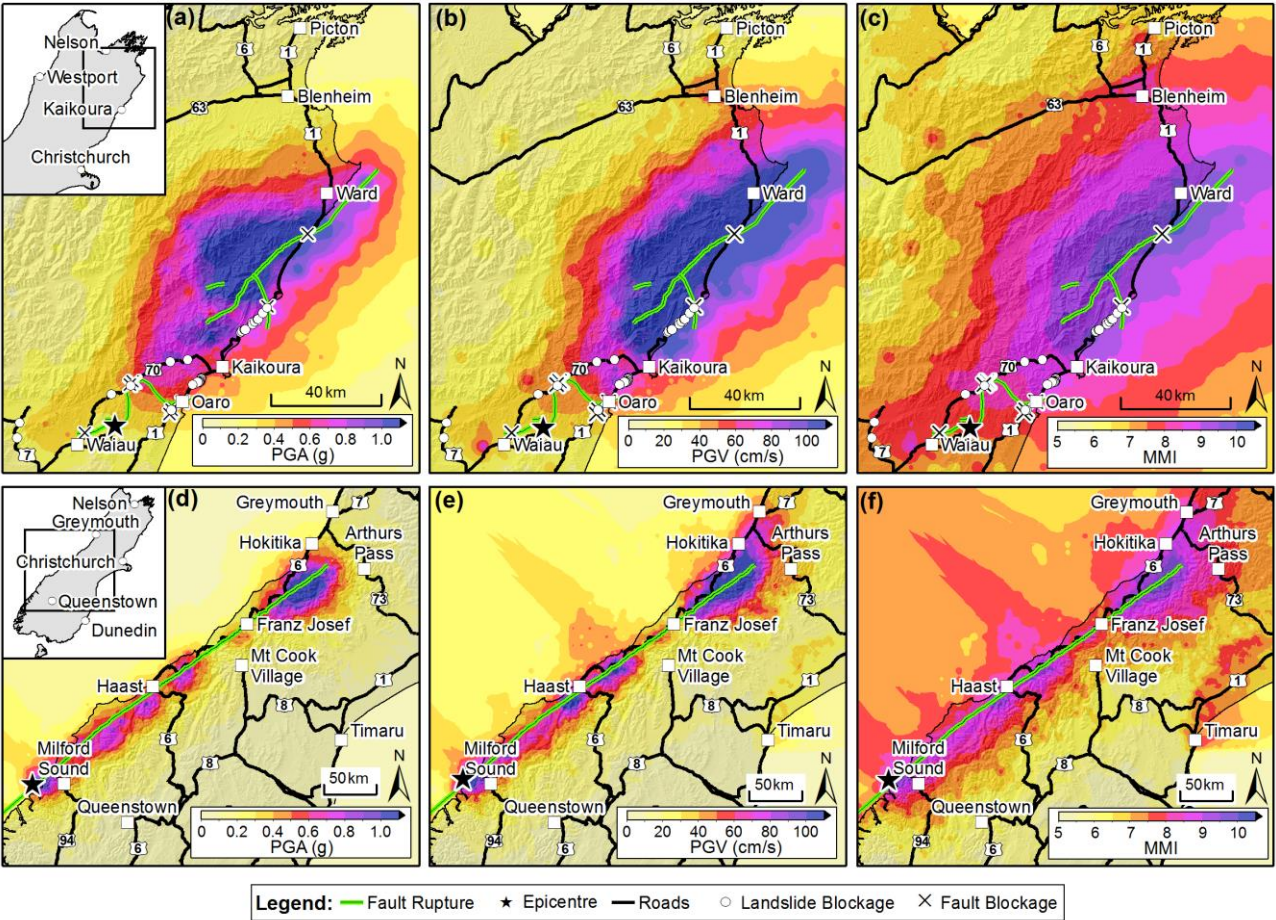


**Figure 1** – Road Impacts and various measures of ground shaking from the 2016  $M_w$  7.8 Kaikōura earthquake (Bradley et al., 2017a) compared to a proposed  $M_w$  7.9 Alpine Fault earthquake scenario rupturing from south to north (Bradley et al., 2017b,c) developed for project AF8 ([www.projectaf8.co.nz](http://www.projectaf8.co.nz)). (a-c) PGA (a), PGV (b) and MMI (c) from the Kaikōura earthquake; (d-e) PGA (d), PGV (e) and MMI (f) for the scenario Alpine Fault earthquake. Inset (a) – location of (a-c) within the upper South Island. Inset (d) – location of (d-f) within the South Island.

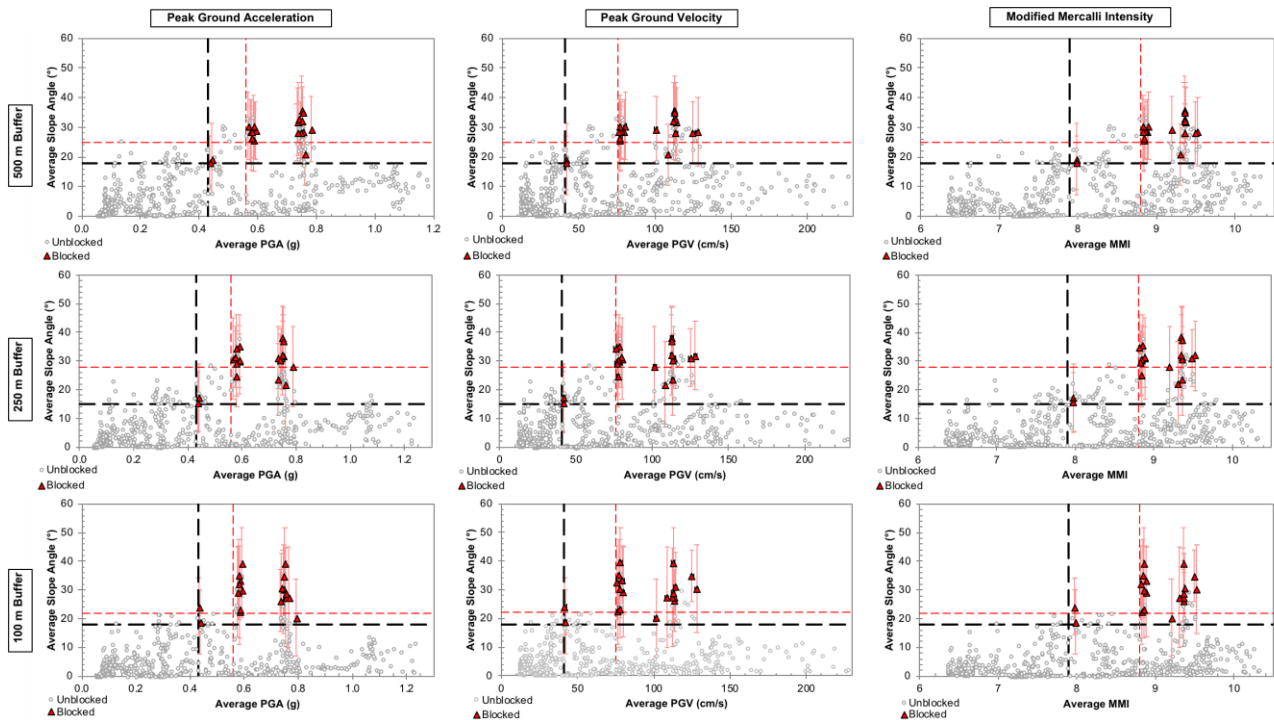


**Figure 2** – Average slope angle compared to average PGA, PGV, and MMI values within 500 m, 250 m, and 100 m buffers for each 500 m section of road network between Christchurch and Picton. Sections blocked by landslides are shown in red with the total range of variable shown by error bars. Sections unaffected by landslides are shown in grey. Black dashed lines represent lower threshold values above which 100% of landslide blockages occur. Red dashed lines represent upper threshold values maximising the number of landslide blockages above the thresholds (true positives) whilst minimising the number of unblocked sections above the thresholds (false positives).

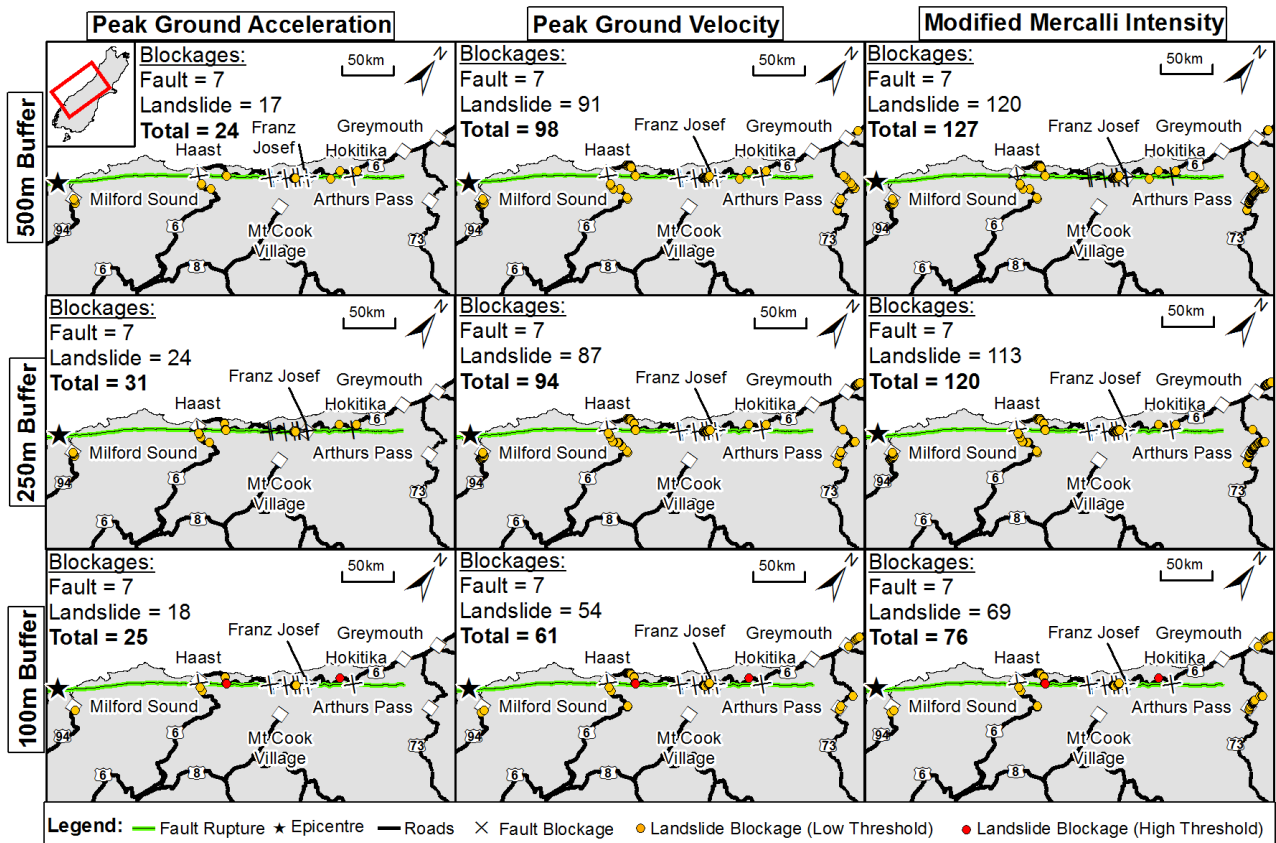


**Figure 3** – Locations of road impacts related to surface fault rupture and landslides from an Alpine Fault earthquake for different buffer widths and shaking variables. Threshold data for landslide blockages are calculated from observations of the Kaikōura earthquake from Fig. 2 and Table 1.



476 **TABLES**

477 **Table 1** – Upper and lower thresholds and corresponding prediction scores derived from Fig. 2 for different buffer widths  
478 and ground shaking variables for landslide road blockages during the 2016 Kaikōura earthquake. TP – true positives,  
479 number of blocked sections above the corresponding thresholds; FP – false positives, number of unblocked sections  
480 above the corresponding thresholds.

	Buffer Width (m)	Shaking Threshold	Slope Threshold	TP (/20)	FP (/634)
PGA (g)	100	0.43	17°	20	20
	250	0.43	17°	20	36
	500	0.43	17°	20	38
	100	0.56	22°	17	10
	250	0.56	28°	15	8
	500	0.56	25°	17	15
PGV (cm/s)	100	41	17°	20	23
	250	41	17°	20	42
	500	41	17°	20	45
	100	76	22°	17	10
	250	76	28°	14	7
	500	76	25°	17	14
MMI	100	7.9	17°	20	24
	250	7.9	17°	20	44
	500	7.9	17°	20	46
	100	8.8	22°	17	10
	250	8.8	28°	15	7
	500	8.8	25°	17	14

481

482